

# Bipartite Entanglement in Out-of-equilibrium Correlated Many-body Systems

Didier Poilblanc<sup>1</sup>

<sup>1</sup> *Laboratoire de Physique Théorique UMR5152, CNRS and Université de Toulouse, F-31062 France*  
(Dated: September 3, 2022)

Thermalization play a central role in out-of-equilibrium physics of ultracold atoms or electronic transport phenomena. On the other hand, entanglement concepts are surprisingly useful to investigate quantum phases of matter. Here, I argue that *bipartite* entanglement measures provide key information on out-of-equilibrium states and offer stringent thermalization criteria. This is illustrated by considering a global quench in an (extended) XXZ spin-1/2 chain across its (zero-temperature) quantum critical point. For non-integrable chains, the entanglement spectrum of the time-averaged *reduced* density matrix of an *extensive subsystem* is shown to closely match the one of a Boltzmann thermal-averaged reduced density matrix.

PACS numbers: 75.10.Jm, 05.30.-d, 05.30.Rt

*Introduction* – Rapid progress in the field of ultracold atoms [1] offer breed new perspectives to realize controlled experimental setup to investigate out-of-equilibrium physics. In particular, real-time observation of quantum dynamics of isolated systems have become possible [2]. In addition, ultracold atoms loaded on optical lattices [1, 3] or laser-cooled Coulomb crystals of charged ions [4] offer very clean experimental implementation of simple lattice many-body Hamiltonians and provide simulators for Condensed Matter. The ability to dynamically change parameters [5] in these Hamiltonians on short time scales could be exploited to realize quantum information processing [1] or cooling [6] devices.

In electronic condensed matter systems, relaxation towards steady states play a central role in many transport phenomena, like e.g. in electric transport resulting from the application of a sudden voltage bias at the edges of a quantum dot [7] or of a Hubbard chain [8]. Spin chains also offers simple generic systems to investigate out-of-equilibrium physics as e.g. in simple physical setup leading to heat transport [9]. However, more generally, thermalization [10] of isolated quantum many-body systems after sudden change of Hamiltonian parameters (quantum quench), a paradigm of out-of-equilibrium dynamics, is still poorly understood, despite recent work on soft-core (Hubbard) [11] and hard-core bosons [12] in one-dimension (1D).

Independently, quantum information concepts have been applied with great success to several domains of Condensed Matter [13], giving new type of physical insights on exotic quantum phases. Quantum entanglement of a A/B bipartition of a many-body (isolated) quantum system can be characterized by the *groundstate* (GS) reduced density matrix  $\rho_A$  obtained from tracing out the B part. The corresponding entanglement Von Neumann (VN) entropy  $S_{VN} = -\text{Tr}\{\rho_A \ln \rho_A\}$  offers an extraordinary tool [14], e.g. to identify one-dimensional systems with underlying conformal field theory (CFT) structure. Another central quantity is the *entanglement spectrum* (ES) defined by the (positive) eigenvalues of a (dimensionless) pseudo-Hamiltonian  $\Xi$  defined by  $\rho_A = \exp(-\Xi)$ . In 1D, the ES reflects faithfully CFT structures [15] or topological symmetries [16]. Non-local real-space partitions have also been used e.g. to define non-local

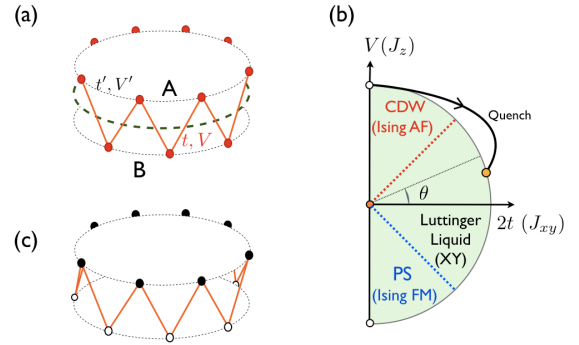


FIG. 1: (Color online) (a) A  $N$ -site (extended) XXZ spin-1/2 chain (drawn here as a "zig-zag" on a periodic ribbon) is partitioned into two identical A and B subsystems of  $L = N/2$  sites by cutting bonds along the dashed line. (b) Phase diagram of the XXZ spin (or hard-core boson) chain mapped onto a circle assuming  $J_{xy} = \cos \theta$  and  $J_z = \sin \theta$ . (c) The CDW groundstate for  $\theta = \pi/2$  i.e.  $t = 0$  ( $J_{xy} = 0$ ) prepared before the quench : all bosons (up spins) are located on A and the B sites are empty (down spins).

order in *gapless* spin chains [17]. Most remarkably, *bipartite* ES universally reflects properties of *edge states* in correlated systems as diverse as fractional quantum Hall states [18] or low-dimensional (ladder) quantum Heisenberg magnets [19].

So far, time evolution of entanglement entropy has been investigated only in very simple cases e.g. for a small block (or segment) in a 1D system after global or local quenches [13, 14]. However, the potential of entanglement measures (such as ES) has not been fully exploited to investigate thermalization of a many-body system. I consider here a *bipartition* (into two halves) of a genuine correlated 1D system (the extended XXZ chain) and the time evolution of the corresponding *reduced* density matrix, ES and entanglement entropy after a global quench, using exact (Lanczos and full) diagonalization techniques. Analysis of such observables shows clearly that the system evolves towards a steady state. Time-average and Boltzmann thermal-average of the *reduced* density matrix are compared. In the non-integrable case, their respective low-energy ES are found to be remarkably similar,

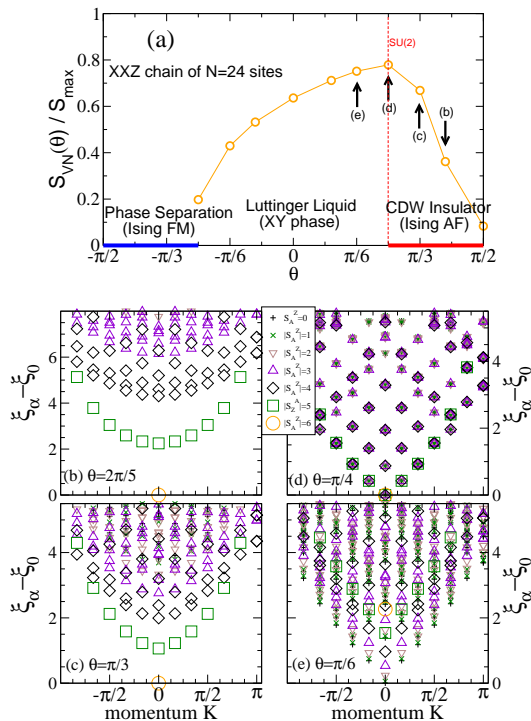


FIG. 2: (Color online) Equilibrium GS properties of the XXZ chain; (a) VN entanglement entropy vs  $\theta$  computed on a  $N=24$  site ring. The entropy is defined *per site* i.e. it is normalized by the maximum value  $S_{\max} = L \ln 2$  ( $L = N/2$ ). (b-e) Typical entanglement *excitation* spectra (for the 4 values of  $\theta$  shown in (b)) as a function of the momentum  $K$  along the ribbon. The eigenvalues  $\xi_\alpha$  of  $\Xi = -\ln \rho_A$  are also labelled according to the Z-component of the total spin (or, equivalently, to the number of bosons  $N_A = L/2 - S_A^z$ ) of the A subsystem and shown by different symbols. Note that, in the CDW phase (LL phase), the doubly-degenerate (unique) "pseudo-GS" of  $\Xi$  (of energy  $\xi_0$ ) carries  $N_A = 0$  or  $N_A = L$  ( $N_A = L/2$ ) hardcore bosons.

providing strong evidence for thermalization.

*Model and setup* – Let us now consider the 1D anisotropic spin-1/2 Heisenberg (so-called XXZ) model (Fig. 1),

$$H = J_z \sum_i S_i^z S_{i+1}^z + \frac{1}{2} J_{xy} (S_i^+ S_{i+1}^- + S_i^- S_{i+1}^+), \quad (1)$$

whose (1D) parameter space can be mapped on a (half) unit circle assuming  $J_{xy} = \cos \theta$  and  $J_z = \sin \theta$ . Alternatively the system can be viewed as a (half-filled) hard-core boson chain with hopping  $t = J_{xy}/2$  and nearest neighbor (NN) repulsion  $V = J_z$ . Its remarkable phase diagram obtained by Haldane [20] and shown in Fig. 1(b) exhibits a Quantum Critical Point (QCP) located exactly at the SU(2)-symmetric point  $\theta = \pi/4$  separating a gapped Charge Density Wave (CDW) insulating phase (Ising phase in the spin language) and a gapless metallic Luttinger Liquid (XY phase). Phase Separation (PS) occurring for an attractive interaction  $|V| > 2t$

( $\theta < -\pi/4$ ) will not be of interest here. Ultimately, we shall consider adding next NN hopping  $t'$  and repulsion  $V'$  (see Fig. 1(a)) in order to break integrability.

In order to construct extensive quantities, it is convenient to realize a very non-local partition of the chain into "even" and "odd" sites. In other words, if the chain is drawn in a zig-zag fashion as in Fig. 1(a), the A and B parts form the two edges of the system which become explicit for  $t' \neq 0$  and  $V' \neq 0$ . One consider here finite chains of  $N$  ( $= 16, 20$  and  $24$ ) sites with periodic boundary conditions, as shown in Fig. 2. The *groundstate* reduced density matrix of the subsystems  $\rho_A = \rho_B$  can be computed using translation symmetry of each  $L = N/2$  site subsystem [19] (each symmetry class is labelled by a momentum  $K = 2\pi n/L$ ) and the conservation of the Z-component of the total spin (i.e. the number of bosons),  $S_A^z + S_B^z = 0$ . Interestingly, liquid and insulating bosonic phases are characterized by qualitatively different entanglement properties. First, the entanglement entropy *per unit length*, shown in Fig. 2(a) for a  $N = 24$  site chain, shows a (kink-like) maximum at the SU(2)-symmetric QCP and vanishes (in the thermodynamic limit) for the classical CDW (Ising) configuration obtained when  $\theta \rightarrow \pi/2$ . Indeed, as shown in Fig. 1(c), for  $\theta = \pi/2$  the (two-fold degenerate) GS is a simple product of a completely filled (A or B) chain by a completely empty (B or A) one. Note that the symmetrized GS (i.e. the equal weight superposition of the two classical GS) still retains a  $1/L$  finite size entropy as shown in Fig. 2(a). Secondly, each quantum phase is uniquely characterized by its ES defined as the spectrum of  $\Xi = -\ln \rho_A$ : Fig. 2(b-c) (Fig. 2(d-e)) for parameters in the CDW phase (LL phase) shows very distinctive features and a clear gapped (linear gapless) spectrum. In addition, at the QCP (Fig. 2(d)) one observes a SU(2) multiplet structure.

*Time evolution* – Let us now consider a *sudden* quantum quench [21] of the system at time  $\tau = 0$ . For simplicity, the initial state  $|\phi(0)\rangle$  is chosen either (i) as one of the two (zero entropy) degenerate GS at  $\theta = \theta_{\text{init}} = \pi/2$  (i.e. for vanishing hopping) shown in Fig. 1(c), where all hardcore bosons are located on a single edge, A or B, or (ii) as a symmetric combination of the two. At times  $\tau > 0$ , the boson hopping  $t$  (spin-flip term in spin language) is switched on, i.e. the value of  $\theta$  discontinuously jumps at  $\tau = 0$  to its "final" value  $\theta_f$  (see Fig. 1(b)). The time evolution of the system wavefunction  $|\phi(\tau)\rangle = \exp(-i\tau H(\theta_f))|\phi(0)\rangle$  is easily computed by (arbitrary) time steps of  $\delta\tau$  (from 0.01 to 0.8) with arbitrary good precision [22] (typically better than  $10^{-16}$ ) by Taylor expanding the time evolution operator  $\exp(-i\delta\tau H(\theta_f))$ . Hence, for finite size systems under consideration, an *exact* computation of the time-dependent reduced density matrix  $\rho_A(\tau) = \text{Tr}_B |\phi(\tau)\rangle\langle\phi(\tau)|$  can be done. Results for the squared-fidelity  $F(\tau) = |\langle\phi(0)|\phi(\tau)\rangle|^2$  and the entanglement entropy  $S_{VN}(\tau) = -\text{Tr}\{\rho_A(\tau) \ln \rho_A(\tau)\}$  are shown in Fig. 3 for increasingly "strong" quenches corresponding to  $\theta_f = 2\pi/5, \pi/3$  and  $\pi/6$ . After a very short transient regime the squared-fidelity drops sharply and the entanglement entropy raises (from zero or  $1/L$ ) to a more or less well defined

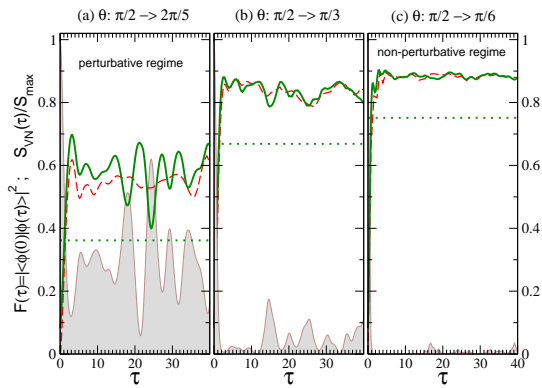


FIG. 3: (Color online) (a-c) Squared-fidelity (shaded) and VN entanglement entropy of various non-equilibrium states obtained after different *sudden* quenches of the  $N = 24$  sites chain Hamiltonian,  $\theta_{\text{init}} \rightarrow \theta_f$  as shown on plots ( $t' = V' = 0$ ). The continuous lines (dashed red line) correspond to a symmetric (non-symmetric) initial state (see text). The dotted (green) line is the GS entropy for  $\theta = \theta_f$ .

plateau, whose average value exceeds the value of the GS of the final Hamiltonian (f-GS). In the  $N \rightarrow \infty$  limit, one expects a non-perturbative regime [23] where  $F(\tau) \sim 2^{-N} \rightarrow 0$ . However, on finite system and for small quench,  $F(\tau)$  can remain large, as seen e.g. in Fig. 3(a). In that regime, integrability of the model can play an important role in the time evolution of the system [24]. Therefore, from now on, one will assume a sufficiently large quench, let say  $\theta_f = \pi/6$ , to observe time evolutions on finite clusters *generic of the thermodynamic limit*. Such a quench corresponds in fact to a quench "across" the QCP at  $\theta = \pi/4$  into the region of stability of the LL phase. However, from Fig. 3(c) we can see a well defined entropy plateau with only small oscillations, suggesting that the system does reach a steady state after the quench. Note also that one finds that non-symmetric and symmetrized initial states give very similar results so that, for simplicity, one can restrict to the symmetric case hereafter.

The time evolution of any (static) observable  $O$  of the  $A$  subsystem is given by  $\tilde{O}(\tau) = \text{Tr}(\rho_A(\tau)O)$ . Time-average like  $\bar{O} = \langle \tilde{O} \rangle$ , where  $\langle G \rangle \equiv \lim_{T \rightarrow \infty} \frac{1}{T} \int_0^T G(\tau) d\tau$ , can then be rewritten as  $\text{Tr}(\rho_A^{\text{ave}} O)$ , involving the *time-averaged* reduced density matrix  $\rho_A^{\text{ave}} = \langle \rho_A \rangle$ . Hence, bipartite entanglement measures can provide precise characterization of the system after the quench, e.g. showing unambiguously it reaches a true steady state. Indeed, one finds that time fluctuations of  $S_{VN}(\tau)$  shown in Fig. 4(a) vanish in the thermodynamic limit (Fig. 4(c)). Interestingly, as seen in Fig. 4(a), we notice that the VN entropy of  $\rho_A^{\text{ave}}$ ,  $S_{VN}^{\text{ave}} = -\text{Tr}\{\rho_A^{\text{ave}} \ln \rho_A^{\text{ave}}\}$ , differs from  $\langle S_{VN} \rangle$ , the time-average of the entanglement entropy. A proper finite size scaling of the two quantities shown in Fig. 4(b) proves that this fundamental property holds in the thermodynamic limit. Incidentally, it is also important

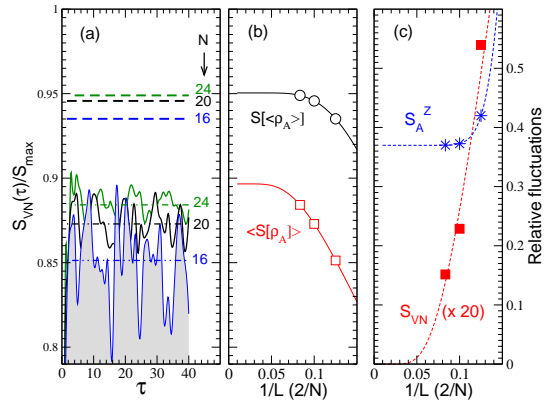


FIG. 4: (Color online) (a) Time-dependent VN entanglement entropy after a *sudden*  $\theta_{\text{init}} = \pi/2 \rightarrow \theta_f = \pi/6$  quench ( $t' = V' = 0$ ), for different chain lengths  $N$  as shown on plots. Dashed-dotted (dashed) lines corresponds to  $\langle S_{VN} \rangle$  ( $S_{VN}^{\text{ave}}$ ). (b) Finite-size scaling of the averages shown in (a). (c) Finite-size scaling of the relative time fluctuations of the entanglement entropy (red squares) and quantum fluctuations of  $S_A^Z$  (normalized by  $L/2$ ). Time-averages are all performed in a  $\Delta\tau = 40$  time interval using a mesh of 50 points (excluding the initial short transient regime). The data of b) and c) are well fitted assuming  $\sim 2^{-\alpha L}$  finite size corrections.

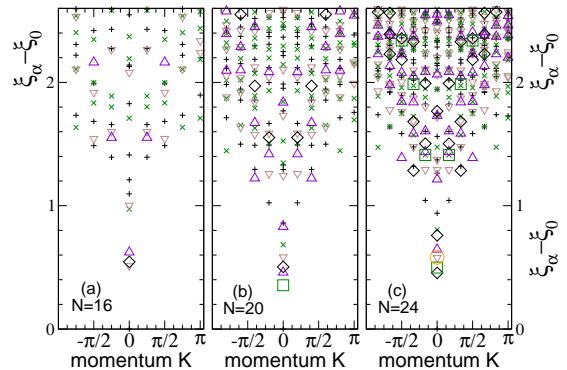


FIG. 5: (Color online) Entanglement spectra of the *time-averaged* reduced density matrix obtained after a  $\theta_{\text{init}} = \pi/2 \rightarrow \theta_f = \pi/6$  quench in XXZ chains of different lengths,  $N = 16, 20$  and  $24$  ( $t' = V' = 0$ ). Symbols are similar to Fig. 2(b-e) and time-averages are performed as for Fig. 4.

to distinguish between "quantum" fluctuations  $\overline{(O - \bar{O})^2} = \text{Tr}\{\rho_A^{\text{ave}}(O - \bar{O})^2\}$  and "time" fluctuations  $\langle (\tilde{O} - \bar{O})^2 \rangle$ . An extreme example is the case of  $S_A^Z$  where  $\tilde{S}_A^Z(\tau) = 0$  at all times (from the time-conserved  $A \leftrightarrow B$  symmetry) while quantum fluctuations are finite as shown in Fig. 4(c).

*Entanglement spectra* – More information on (bipartite) entanglement in the steady state is provided by the ES of  $\rho_A^{\text{ave}}$ .

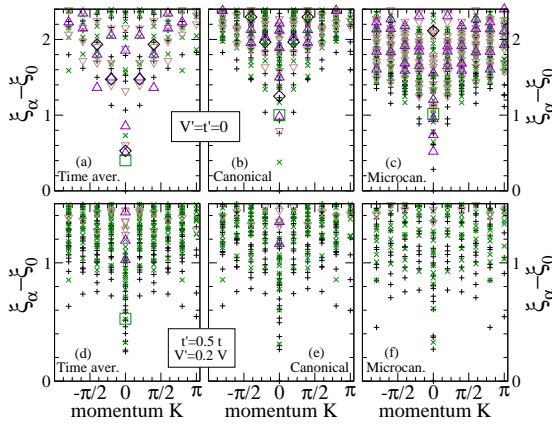


FIG. 6: (Color online) ES of  $\rho_A^{\text{ave}}$  (a,d),  $\rho_A^{\text{can}}$  (b,e) and  $\rho_A^{\text{micro}}$  (c,f) obtained by *full diagonalization* of  $N = 20$  site integrable ( $t' = V' = 0$ ) and non-integrable chains ( $\theta_{\text{init}} = \pi/2 \rightarrow \theta_f = \pi/6$  quench). Symbols are similar to Fig. 2(b-e).  $1/\beta \simeq 2.07$  (b),  $\Delta E = 0.3$  (c),  $1/\beta \simeq 1.48$  (e) and  $\Delta E = 0.1$  (f).

The latter computed for XXZ chains with 16, 20 and 24 sites, and shown in Fig. 5(a-c), reveal a smooth convergence with system size, an accumulation of low pseudo-energy levels at  $K = 0$  and a small pseudo-energy gap, in sharp contrast with the ES of the f-GS shown in Fig. 2(e). In fact, further considerations based on the reduced density matrix  $\rho_A$  offer stringent thermalization criteria. Indeed, thermal averages of  $\rho_A$  can be performed (now requiring the full diagonalization of  $H(\theta_f)$ ) and compared to  $\rho_A^{\text{ave}}$ :

$$\rho_A^\lambda = \sum_\alpha w_\alpha^\lambda \text{Tr}_B |\Psi_\alpha\rangle\langle\Psi_\alpha|, \quad (2)$$

where the prime means the sum is restricted to eigenstates of  $H(\theta_f)$  with *non-zero* overlap with  $|\phi(0)\rangle$ , accounting for conserved quantities like momentum, z-component of total spin, etc... The *infinite-time* average  $\rho_A^{\text{ave}}$ , depends on the initial state via  $w_\alpha^{\text{ave}} = |\langle\Psi_\alpha|\phi(0)\rangle|^2$ , in contrast to canonical ( $w_\alpha^{\text{can}} = \frac{1}{Z} \exp(-\beta E_\alpha)$  where  $E_\alpha$  are eigenenergies associated to  $|\Psi_\alpha\rangle$ ) and microcanonical ( $w_\alpha^{\text{micro}} = \text{Cst}$  in an energy window  $[E_0 - \Delta E, E_0 + \Delta E]$ ) thermal averages. Note, the effective temperature  $1/\beta$  of the canonical ensemble is (implicitly) given by constraining the conserved mean-energy to be  $E_0 = -(V - V')L/2$ . Results shown in Figs. 6 reveal fundamental differences between integrable and non-integrable Hamiltonians. For the latter, surprisingly good agreement between the low-energy ES of  $\rho_A^{\text{ave}}$  and  $\rho_A^{\text{can}}$  is seen, suggesting an extension of the *eigenstate thermalization scenario* [10] to bipartite entanglement properties of eigenstates. In contrast, for the plain integrable XXZ chain, important differences between the various averages reveal incomplete thermalization.

To summarize, the concept of bipartite entanglement in out-of-equilibrium many-body systems is introduced and shown to provide stringent probes of thermalization. This approach

enables to show that thermalization in non-integrable systems occurs even up to the level of the reduced density matrix of an *extensive* subsystem.

*Acknowledgements* – I thank D. Braun, B. Georgeot, T. Lahaye, I. Nechita, P. Pujol, N. Regnault, M. Rigol, G. Roux and K. Ueda for interesting discussions, IDRIS (Orsay, France) for CPU time on the NEC-SX8 supercomputer and the French Research Council (ANR) for funding.

- 
- [1] Dieter Jaksch and Stephen A. Clark, *Cold Atoms in Optical Lattices*, 1st Edition., 2010, IV, 300 p., Springer, Germany & Canopus Academic Publishing Limited, UK.
  - [2] T. Kinoshita, T. Wenger, D. S. Weiss, *Nature* **440**, 693 (2006).
  - [3] D. Jaksch, C. Bruder, J. I. Cirac, C. W. Gardiner, and P. Zoller, *Phys. Rev. Lett.* **81** 3108 (1998); R. Jördens, N. Strohmaier, K. Günter, H. Moritz, and T. Esslinger, *Nature* **455**, 204 (2008).
  - [4] M. Johanning, A. F. Varón, and C. Wunderlich, *J. Phys. B: At. Mol. Opt. Phys.* **42**, 154009 (2009).
  - [5] M. Greiner, O. Mandel, T. Esslinger, T. W. Hansch and I. Bloch, *Nature* **415**, 39 (2002).
  - [6] F. Heidrich-Meisner et al., *Phys. Rev. A* **80**, 041603(R) (2009).
  - [7] S. Kirino, T. Fujii, J.Z. Zhao and K. Ueda, *J. Phys. Soc. Jpn* **77**, 084704 (2008); F. Heidrich-Meisner, A. E. Feiguin, and E. Dagotto, *Phys. Rev. B* **79**, 235336 (2009).
  - [8] S. Kirino and K. Ueda, *J. Phys. Soc. Jpn* **79**, 093710 (2010); F. Heidrich-Meisner et al., *Phys. Rev. B* **82**, 205110 (2010).
  - [9] M. Michel, G. Mahler, and J. Gemmer, *Phys. Rev. Lett.* **95**, 180602 (2005).
  - [10] M. Rigol, V. Dunjko, and M. Olshanii, *Nature* **452**, 854 (2008).
  - [11] C. Kollath, A. M. Läuchli, and E. Altman, *Phys. Rev. Lett.* **98**, 180601 (2007); G. Roux, *Phys. Rev. A* **79**, 021608(R) (2009).
  - [12] M. Rigol, *Phys. Rev. Lett.* **103**, 100403 (2009); M. Rigol and L. F. Santos, *Phys. Rev. A* **82**, 011604(R) (2010).
  - [13] L. Amico, R. Fazio, A. Osterloh, and V. Vedral, *Rev. Mod. Phys.* **80**, 517 (2008).
  - [14] *Special Issue: Entanglement Entropy in Extended Quantum Systems*, *J. Phys. A* **42**, N° 50, 500301-504012 (2009); Guest Editors: P. Calabrese, J. Cardy and B. Doyon.
  - [15] P. Calabrese and A. Lefevre, *Phys. Rev. A* **78**, 032329 (2008).
  - [16] Franck Pollmann, Ari M. Turner, Erez Berg, and Masaki Oshikawa, *Phys. Rev. B* **81**, 064439 (2010).
  - [17] Ronny Thomale, D. P. Arovas, and B. Andrei Bernevig, *Phys. Rev. Lett.* **105**, 116805 (2010).
  - [18] Hui Li and F. D. M. Haldane, *Phys. Rev. Lett.* **101**, 010504 (2008); N. Regnault, B. A. Bernevig, F. D. M. Haldane, *Phys. Rev. Lett.* **103**, 016801 (2009); A.M. Läuchli, E. J. Bergholtz, J. Suorsa, and M. Haque, *Phys. Rev. Lett.* **104**, 156404 (2010); R. Thomale, A. Sterdyniak, N. Regnault, and B. A. Bernevig, *Phys. Rev. Lett.* **104**, 180502 (2010).
  - [19] D. Poilblanc, *Phys. Rev. Lett.* **105**, 077202 (2010).
  - [20] F. D. M. Haldane, *Phys. Rev. Lett.* **45**, 1358 (1980).
  - [21] For continuous quenches see EPAPS Document No. XXX. For more information on EPAPS, see <http://www.aip.org/pubservs/epaps.html>.
  - [22] G. Roux, *PhD Thesis*, Université Paul Sabatier - Toulouse III (2007), <http://tel.archives-ouvertes.fr/tel-00167129>.
  - [23] G. Roux, *Phys. Rev. A* **81**, 053604 (2010).
  - [24] F. Mila and D. Poilblanc, *Phys. Rev. Lett.* **76**, 287 (1996).

**Supplementary material to**  
**Bipartite Entanglement in Out-of-equilibrium Correlated Many-body**  
**Systems**

Didier Poilblanc<sup>1</sup>

<sup>1</sup> *Laboratoire de Physique Théorique UMR5152,  
CNRS and Université de Toulouse, F-31062 France*

arXiv:1011.2147v3 [cond-mat.str-el] 2 Dec 2010

This supplement of the main paper provides additional data for the case of continuous quenches of the Hamiltonian parameters.

### Quasi-adiabatic quenches

As shown in the main paper, the system after the quench possesses an excess of entanglement entropy (per unit length) compared to the f-GS. There is in fact an interesting correlation between this excess entropy and the "speed" at which the quench is performed. A smooth quench can be realized by considering a time-dependent Hamiltonian  $H(\theta(\tau))$  where  $\theta(\tau)$  decreases continuously from  $\theta_{\text{init}} = \pi/2$  to  $\theta_f = \pi/6$  in a time-interval  $[0, T_f]$ . One can choose e.g.

$$\theta(\tau) = (1 - \tilde{w}_\tau)\theta_{\text{init}} + \tilde{w}_\tau\theta_f, \quad (1)$$

$$\tilde{w}_\tau = (w_\tau - w_0)/(w_{T_f} - w_0), \quad (2)$$

$$w_\tau = 1/(1 + \exp((T_f/2 - \tau)/T_1)), \quad (3)$$

and  $T_1 = T_f/10$ . As shown in Fig. 1, under increasing the characteristic time  $T_1$  the average value of the entropy plateau decreases towards the GS value, as expected for increasingly adiabatic processes. Interestingly, the deviation  $\langle S_{\text{VN}} \rangle - S_{\text{VN}}^{\text{ave}}$  also simultaneously decreases (to reach zero for a fully adiabatic process).

Sudden and continuous quenches also give very different ES of the time-averaged reduced density matrix  $\rho_A^{\text{ave}}$ . Data for continuous and sudden quenches are compared in Fig. 2. Remarkably, the spectra in the quasi-adiabatic case resemble very closely the equilibrium f-GS spectrum of Fig. 2(e) of the main paper with a clear linear envelope, in contrast to the spectra obtained for a sudden quench. However, we note that the requirement (e.g. on the time scale  $T_1$ ) to have a quasi-adiabatic process becomes more and more stringent for increasing system size because of the vanishing of the finite-size gap (in the XY phase).

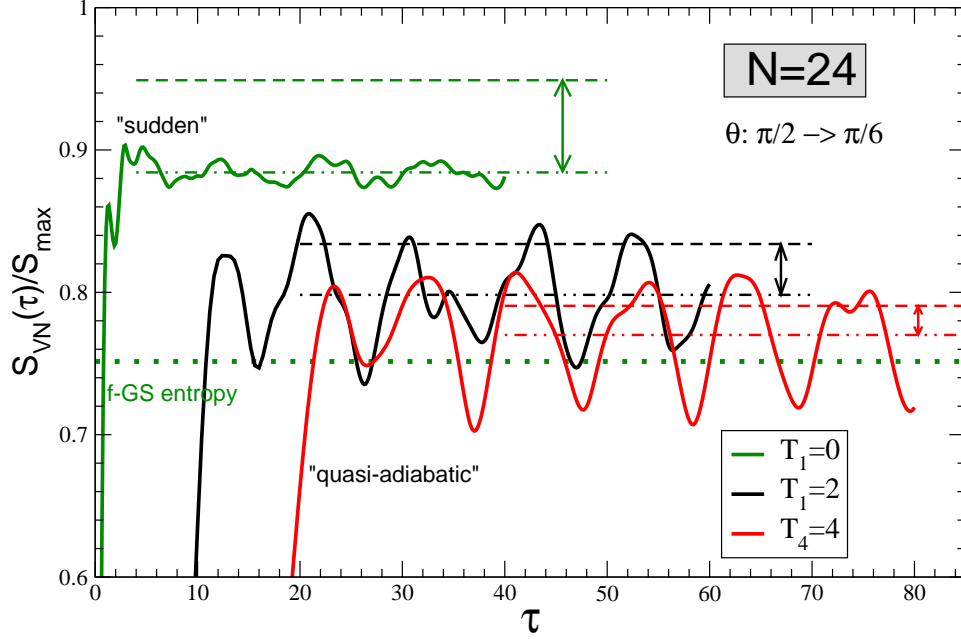


FIG. 1: (Color online) VN entanglement entropy of various non-equilibrium states obtained after a  $\theta_{\text{init}} = \pi/2 \rightarrow \theta_f = \pi/6$  quench realized on a 24-site XXZ chain ( $t' = V' = 0$ ) over different time scales characterized by  $T_1$ . The arrows indicate the difference between the time-averaged entropy  $\langle S_{\text{VN}} \rangle$  (dot-dashed lines) and the VN entropy of  $\rho_A^{\text{ave}}$ ,  $S_{\text{VN}}^{\text{ave}}$  (dashed lines). Time-averages have been performed using 50 bins in a  $\Delta\tau = 40$  time-interval within the plateaux.

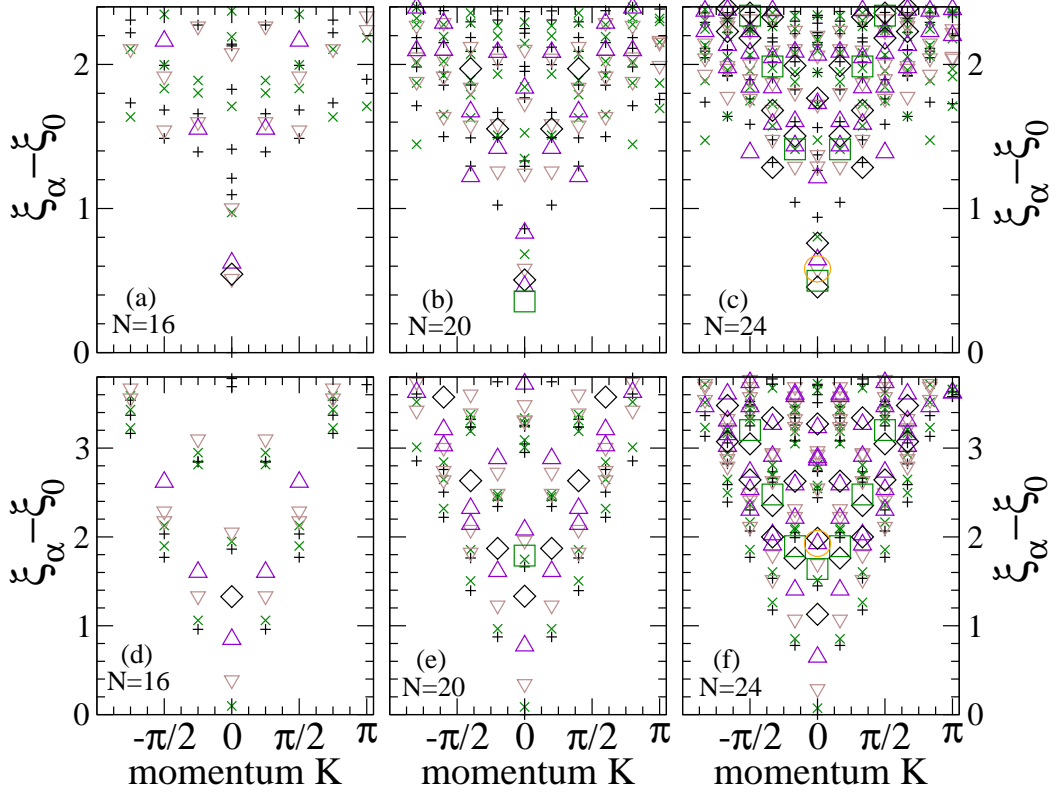


FIG. 2: (Color online) Entanglement spectra of *time-averaged* reduced density matrices in XXZ chains of different lengths,  $N = 16, 20$  and  $24$  ( $t' = V' = 0$ ). Same symbols as in main paper and same procedure for time averaging as above and in main paper. Comparison between a sudden quench (a-c) and a quasi-adiabatic  $T_1 = 4$  quench (d-f). In both cases,  $\theta_{\text{init}} = \pi/2 \rightarrow \theta_{\text{f}} = \pi/6$ .